Z. Phys. D - Atoms, Molecules and Clusters 22, 701-711 (1992)

Atoms, Molecules
Zeitschrift für Physik D and Clusters

Second-order theories for electron loss in fast collisions with He atoms

D.H. Jakubaßa-Amundsen

Sektion Physik, Universität München, Am Coulombwall 1, W-8046 Garching, Federal Republic of Germany

Received August 15, 1991

Abstract. The momentum distribution of projectile electrons ejected in collisions with light targets is calculated within the second-order Born approximation for direct ionisation and within the electron impact approximation and the impulse approximation for electron capture to the target continuum. From comparison with available experimental data it is found that for forward emission angles the electron is well described by a projectile eigenstate, while at backward angles a target final state is more appropriate. At all angles the inclusion of simultaneous target excitation is very important.

PACS: 34.50.Fa

1. Introduction

It is now generally accepted that electron ejection from energetic projectiles cannot to sufficient accuracy be described by the first-order Born approximation for direct ionisation. Even when simultaneous target excitation is taken into consideration, this theory provides only a qualitative explanation of the electron loss peak which appears at electron momenta k_f close to the collision velocity v [1]. Deviations from the first Born approximation manifest themselves in the shape of the forward peak at zero emission angle [2, 3], where the cusp asymmetry is a direct measure of the higher-order couplings of the electron to the target field [4]. At larger emission angles, the first Born approximation fails to reproduce the high intensity at the low-energy side of the loss peak which has been measured for electrons detected in coincidence with charge-changed projectiles [5–7]. This additional intensity has been attributed to simultaneous target excitation which results not only from the electron-electron interaction (the so-called 'coherent' projectile-target ionisation), but also from the projectile nucleus-target electron interaction ('incoherent' projectile-target ionisation) [6].

In this work the loss theories valid for $Z_p \sim Z_T$ and $v > Z_P$ (where Z_P and Z_T are the nuclear charges of projectile and target, respectively) are revisited and extended to account for second-order effects in both the elastic and the inelastic contributions to the doubly differential cross section. Here, elastic and inelastic refer to a ground-state and excited target in the final state, respectively. Due to the difficulty of describing the simultaneous influence of the projectile and the target field on the ejected electron, either a projectile or a target eigenstate will be chosen. For small relative momenta between the continuum electron and the projectile, i.e. for forward emission angles, the influence of the target field is small, and the second-order Born approximation for direct ionisation has been found to provide a satisfactory description for He targets in the cusp region [4], and at forward angles up to 50° [8]. In the present work, the Born approximation is also applied to backward angles using, however, a new closure approximation for the evaluation of the inelastic contribution, which particularly accounts for a proper description of target ionisation [9].

When the electron is ejected into the backward hemisphere, the target potential gains increasingly influence on the electron. This may be accounted for by either allowing for intermediate target eigenstates as has been done by Hartley and Walters [10] in the framework of the impulse approximation, or by forcing the electron into a final target state like in the electron impact approximation (EIA) [11] which is basically the Brinkman-Kramers theory for rearrangement. Both theories have originally been formulated for heavy targets with $Z_P \ll Z_T$, and they do not account for the incoherent projectile-target ionisation. The EIA which only considers the elastic contribution to the loss cross section, has recently also been applied to He targets [12], but the agreement with experiment is not very satisfactory. In the present work, the EIA is improved in two ways: first, the inelastic contribution from the incoherent projectile-target ionisation is added. This should be a good description for backward angles where the coherent projectile-target ionisation is considered to be small [10]. Second, accounting

for the fact that a proper description of rearrangement requires a higher-order theory [13, 14], the EIA is combined with the second-order term to the prior impulse approximation (IA), and in the same framework, target excitation by electron-electron coupling is accounted for in addition to the incoherent contribution. Since the IA includes intermediate projectile eigenstates, its validity is expected to extend to smaller emission angles as compared to the EIA.

The paper is composed in the following way. In Sect. 2, the second Born approximation with the new closure approximation is shortly presented. Section 3 describes the electron impact approximation including the incoherent part of the target excitation. In Sect. 4, the impulse approximation is derived. Numerical details are given in Sect. 5. The comparison of the theoretical results with experimental data for He^+, He^0 and H^0 projectiles is performed in Sect. 6 and the conclusion is drawn in Sect. 7. Atomic units ($\hbar = m = e = 1$) are used unless otherwise indicated.

2. The second Born approximation (B2)

For the formal presentation of the theories, we restrict ourselves to a one-electron projectile and a neutral target. The multi-electron target states, denoted by ϕ^T, will be described by Slater determinants of single-particle Hartree-Fock states. The electronic projectile states ψ^P are hydrogenlike, while the scattering states ψ^T of the electron in the field of the neutral target are solutions of an appropriate single-particle Schrödinger equation. The semiclassical approximation with a straight-line internuclear trajectory, $\mathbf{R} = \mathbf{b} + \mathbf{v}t$, with impact parameter b, will be used.

In the initial channel, and for the Born approximation throughout, the Hamiltonian is split in the following way

$$H = H_{oi} + V_i$$

$$H_{oi} = H_T + T_e + V_{Po}, \qquad V_i = V_{ee} + V_{Pe} + V_{eT} \tag{2.1}$$

where H_{oi} is the electronic Hamiltonian for the separated projectile-target system, with H_T the target Hamiltonian and T_e the kinetic energy of the projectile electron. V_{ee} is the projectile electron-target electron interaction, V_{Po} and V_{eT} the couplings between the projectile electron and the projectile and target nuclear fields, respectively, and V_{Pe} is the interaction between the projectile nucleus and the target electrons. Explicitly, for an N-electron target, the potentials are given by

$$V_{ee} = \sum_{n=1}^{N} \frac{1}{|\mathbf{r}_T - \mathbf{r}_{nT}|}, \qquad V_{Po} = -\frac{Z_P}{r_P}, \qquad V_{eT} = -\frac{Z_T}{r_T}$$

$$V_{Pe} = -Z_P \sum_{n=1}^{N} \frac{1}{|\mathbf{r}_{nT} - \mathbf{R}|} \tag{2.2}$$

where the electronic coordinates are displayed in Fig. 1. In the second-order Born approximation, the transition amplitude for exciting the projectile electron from ψ_i^P (with energy ε_i^P) to ψ_f^P (with energy ε_f^P) and the target from ϕ_i^T (with energy E_i^T) to ϕ_f^T (with energy E_f^T) reads

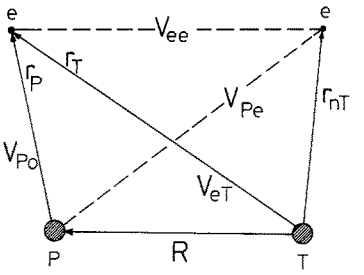

Fig. 1. Coordinates and interaction potentials for the collision system consisting of the projectile nucleus (P), the target nucleus (T) and the electrons (e). Only one target electron is shown

$$a_{fi}^{B2} = -i \int_{-\infty}^{\infty} \mathrm{d}t \, \langle \phi_f^T \psi_f^P | \, V_i + V_i G_{oi} V_i | \phi_i^T \psi_i^P \rangle \tag{2.3}$$

where the choice of propagation in the projectile field, $G_{oi} = (i\partial_t - H_{oi} + i\varepsilon)^{-1}$, restricts the applicability of the Born theory (2.3) to systems with $Z_P \gtrsim Z_T$. Since a detailed description of the theory has been given earlier [4], it shall only be pointed out that in the second-order term the one-electron approximation to V_{ee} is made,

$$V_{ee} + V_{eT} \to V_T \equiv \langle \phi_i^T | \, V_{ee} | \phi_i^T \rangle + V_{eT} \tag{2.4}$$

which is the more appropriate, the larger Z_P and Z_T. This leads to the following formulae for the elastic ($\phi_f^T = \phi_i^T$) and inelastic ($\phi_f^T \neq \phi_i^T$) part of the transition amplitude

$$\begin{aligned} a_{fi}^{B2,\,\mathrm{el}} = & -i \int \mathrm{d}t \langle \psi_f^P | \, V_T | \psi_i^P \rangle \\ & - i \int \mathrm{d}t \langle \phi_i^T \psi_f^P | \, V_T G_{oi} V_T | \phi_i^T \psi_i^P \rangle \end{aligned} \tag{2.5}$$

$$\begin{aligned} a_{fi}^{B2,\,\mathrm{in}} = & -i \int \mathrm{d}t \langle \phi_f^T \psi_f^P | \, V_{ee} | \phi_i^T \psi_i^P \rangle \\ & - i \int \mathrm{d}t \langle \phi_f^T \psi_f^P | \, V_{Pe} G_{oi} V_T + V_T G_{oi} V_{Pe} | \phi_i^T \psi_i^P \rangle . \end{aligned}$$

The inelastic part consists of two contributions, the first-order term mediated by V_{ee} (the coherent ionisation) and the second-order term based on two successive interactions between an electron of one atom and the central field of the other (the incoherent ionisation). Hence, the inelastic contribution to the doubly differential cross section for the ejection of electrons with an energy $E_f = k_f^2/2$ into the solid angle $\mathrm{d}\Omega_f$ (in the target frame of reference) has the following structure

$$\frac{\mathrm{d}^2\sigma^{\mathrm{in}}}{\mathrm{d}E_f \mathrm{d}\Omega_f} = \frac{4k_f}{v} \sum_{f>N} \int \mathrm{d}\mathbf{q} \, \delta(\Delta E_{fi} - \mathbf{q}\mathbf{v}) \, F_f(\mathbf{q})$$

$$\begin{aligned} F_f(\mathbf{q}) = \sum_{n=1}^{N} | \langle \varphi_f^T | \, & \mathrm{e}^{\mathrm{i}\mathbf{q}_1 \mathbf{r}_{nT}} M^{\mathrm{coh}}(\mathbf{q}) \\ & + \mathrm{e}^{\mathrm{i}\mathbf{q}_2 \mathbf{r}_{nT}} M^{\mathrm{inc}}(\mathbf{q}) | \varphi_n^T \rangle |^2 \end{aligned} \tag{2.6}$$

where $\{\varphi_n^T\}$ are the initially occupied Hartree Fock target orbitals and the sum over final target states f

runs over all excited states above the Fermi level. The total excitation energy of the system is denoted by $\Delta E_{fi}=\varepsilon_f^P-\varepsilon_i^P+E_f^T-E_i^T$, and $\mathbf{q}_1$ and $\mathbf{q}_2$ are two electronic momenta which may depend on $\mathbf{q}$. The matrix elements of the coherent and incoherent ionisation are denoted by M^{coh} and M^{inc}, respectively, and are given in [4]. The factorisation of the incoherent contribution into an $\mathbf{r}_{nT}$-independent matrix element $M^{\mathrm{inc}}(\mathbf{q})$ times an exponential $\mathbf{r}_{nT}$ dependence is made possible by an additional peaking approximation.

Two closure approximations for the simplification of the sum over final target states will be discussed. The first one, which is commonly used, relies on the replacement of the target excitation energy by some average value [15]

$$\Delta E_{fi}^T\equiv E_f^T-E_i^T\to I^T+\varepsilon_f^P \tag{2.7}$$

where I^T is the ionisation potential of the target (the K-shell binding energy in case of He) and $\varepsilon_f^P=\kappa_f^2/2$ with $\boldsymbol{\kappa}_f=\mathbf{k}_f-\mathbf{v}$ the electron momentum in the projectile reference frame. As a consequence, completeness of the target states can be used to evaluate the sum over f. For a He target, the result is

$$\begin{aligned}F(\mathbf{q})&\equiv\sum_{f>N}F_f(\mathbf{q})\\&=|M^{\mathrm{coh}}(\mathbf{q})|^2S_{\mathrm{in}}(q_1)+|M^{\mathrm{inc}}(\mathbf{q})|^2S_{\mathrm{in}}(q_2)\\&\quad+2\,\mathrm{Re}\{M^{\mathrm{coh}*}(\mathbf{q})M^{\mathrm{inc}}(\mathbf{q})\}\\&\quad\times[F_{\mathrm{el}}(|\mathbf{q}_1-\mathbf{q}_2|)-\tfrac{1}{2}F_{\mathrm{el}}(q_1)F_{\mathrm{el}}(q_2)]\end{aligned} \tag{2.8}$$

where $S_{\mathrm{in}}(q)$ is the incoherent scattering form factor which for a He target is related to the elastic form factor $F_{\mathrm{el}}(q)$ by means of $S_{\mathrm{in}}(q)=2-F_{\mathrm{el}}^2(q)/2$ [16]. The form factors are tabulated for most targets; equivalently, $F_{\mathrm{el}}(q)$ can be calculated from the Fourier transformed target atomic potential [4, 17].

The second way for the evaluation of the sum over f relies on the fact that for electron loss, target excitation to the continuum plays an important role. Hence, the sum over f is replaced by an integral over target electron momenta $\boldsymbol{\kappa}_T$, and φ_f^T represents the corresponding continuum eigenstates. Accounting for the contribution of the bound excited target states by a renormalisation constant c_T, one has from (2.6) [9]

$$\begin{aligned}\frac{\mathrm{d}^2\sigma^{\mathrm{in}}}{\mathrm{d}E_f\,\mathrm{d}\Omega_f}&=\frac{4k_f}{v}\int_0^\infty\kappa_T^2\mathrm{d}\kappa_T\int\mathrm{d}\mathbf{q}\,\delta(\Delta E_{fi}-\mathbf{qv})\,c_T\\&\quad\times\int\mathrm{d}\Omega_\kappa F_f(\mathbf{q})\end{aligned} \tag{2.9}$$

where $\Delta E_{fi}^T=I^T+\kappa_T^2/2$, and c_T is determined from the requirement that for $\kappa_T^2/2\to\varepsilon_f^P$, (2.9) should coincide with the result from the conventional closure approximation (2.6) with (2.8). The evaluation of (2.9) does not meet particular difficulties when either the coherent or incoherent contribution is dropped, because then the angular integral over $\mathrm{d}\Omega_\kappa$ can be carried out analytically. Due to the interference term between M^{coh} and M^{inc}, this is, however, no longer possible in the general case. In order to keep the theory tractable we drop the interference term in $F_f(\mathbf{q})$ but retain it in c_T, such that for a fixed average target excitation energy, the conventional closure approximation is recovered. Since the matrix elements $M^{\mathrm{coh}}(\mathbf{q})$ and $M^{\mathrm{inc}}(\mathbf{q})$ are independent of Ω_κ, this leads to the approximation

$$\begin{aligned}&c_T\int\mathrm{d}\Omega_\kappa F_f(\mathbf{q})\\&\quad=F(\mathbf{q})\,\frac{|M^{\mathrm{coh}}(\mathbf{q})|^2\bar{G}(\kappa_T,q_1)+|M^{\mathrm{inc}}(\mathbf{q})|^2\bar{G}(\kappa_T,q_2)}{|M^{\mathrm{coh}}(\mathbf{q})|^2\bar{S}(q_1)+|M^{\mathrm{inc}}(\mathbf{q})|^2\bar{S}(q_2)}\\&\bar{G}(\kappa_T,q)=\int\mathrm{d}\Omega_\kappa\sum_{n=1}^N|\langle\varphi_f^T|\mathrm{e}^{\mathrm{i}\mathbf{qr}}|\varphi_n^T\rangle|^2\\&\bar{S}(q)=\int_0^\infty\kappa_T^2\mathrm{d}\kappa_T\bar{G}(\kappa_T,q)\end{aligned} \tag{2.10}$$

with $F(\mathbf{q})$ from (2.8). If in the expression for $\bar{G}(\kappa_T,q)$, φ_n^T is approximated by a hydrogenlike $1s$ state with an effective charge Z ($Z=1.7$ for He), the angular integral in $\bar{G}(\kappa_T,q)$ is easily carried out with the result (for $N=2$) [9]

$$\begin{aligned}\bar{G}(\kappa_T,q)&=\frac{2^9Z^6q^2}{\kappa_T(1-\mathrm{e}^{-2\pi\eta})}\,|[q^2-(\kappa_T+\mathrm{i}Z)^2]^{-\mathrm{i}\eta}|^2\\&\quad\times\frac{q^2+\frac{1}{3}(Z^2+\kappa_T^2)}{[(Z^2+q^2+\kappa_T^2)^2-4q^2\kappa_T^2]^3}\end{aligned} \tag{2.11}$$

with $\eta=Z/\kappa_T$. The approximations involved in the derivation of (2.10) and (2.11) are not expected to be of serious consequence because they affect numerator and denominator of $c_T\int\mathrm{d}\Omega_\kappa F_f(\mathbf{q})$ in a similar way. The advantage of this Hartley-Walters closure approximation is the absence of a free parameter (the mean excitation energy) and the excellent agreement with accurate calculations for the first Born approximation ($M^{\mathrm{inc}}=0$) [9]. It will be used in all theories discussed below.

3. The electron impact approximation (EIA)

In this approximation the ejected electron is described by a target eigenstate. Consequently, in the final channel the Hamiltonian is split according to

$$\begin{aligned}H&=H_{of}+V_f\\H_{of}&=H_T+T_e+V_T,\\V_f&=V_{ee}-\langle V_{ee}\rangle+V_{Pe}+V_{Po}\end{aligned} \tag{3.1}$$

with $\langle V_{ee}\rangle=\langle\phi_i^T|V_{ee}|\phi_i^T\rangle$ and V_T from (2.4). The exact transition amplitude for this rearrangement process is given by

$$a_{fi}=-\mathrm{i}\int_{-\infty}^{\infty}\mathrm{d}t\langle\phi_f^T\psi_f^T|V_i+V_fGV_i|\phi_i^T\psi_i^P\rangle \tag{3.2}$$

with $G=(\mathrm{i}\partial_t-H+\mathrm{i}\varepsilon)^{-1}$ the full propagator of the system. The second-order approximation to a_{fi} is obtained by dropping V_i or V_f in G. In the elastic contribution, the

replacement $G \to G_{oi}$ is made like in the second Born approximation (2.3). Applying the one-electron approximation, i.e. setting $V_{ee} - \langle V_{ee} \rangle = 0$ in the second-order term, one obtains

$$a_{fi}^{\mathrm{el}} = -i \int \mathrm{d}t \langle \phi_i^T \psi_f^T | (1 + V_{Po} G_{oi}) \times (V_T + V_{Pe}) | \phi_i^T \psi_i^P \rangle . \tag{3.3}$$

The contribution from $V_{Pe} G_{oi} (V_T + V_{Pe})$ has been dropped because $V_{Pe} G_{oi} V_T$ does not lead to target ground state-ground state scattering, while the matrix element of $V_{Pe} G_{oi} V_{Pe}$ is proportional to the overlap between ψ_f^T and ψ_i^P and hence small for large collision velocities.

For the coherent contribution to inelastic scattering, the same replacement, $G \to G_{oi}$ will be made, since this contribution is basically important for small ejection angles and small momentum transfers where the projectile field is supposed to have the dominant influence on the electronic intermediate states. For the incoherent contribution, however, which is dominant at backward emission angles, the choice $G \to G_{of} = (i\partial_t - H_{of} + i\varepsilon)^{-1}$ will be made. This choice has two additional advantages, first, the restriction $Z_T \lesssim Z_P$ can be dropped, and second, the further evaluation is much less involved than it would be with the replacement $G \to G_{oi}$. Setting $V_{ee} \approx \langle V_{ee} \rangle$ in the incoherent term, one has

$$\begin{aligned} a_{fi}^{\mathrm{in}} = & -i \int \mathrm{d}t \langle \phi_f^T \psi_f^T | (1 + V_{Po} G_{oi}) \\ & \times (V_{ee} + V_{Pe} + V_{eT}) | \phi_i^T \psi_i^P \rangle \\ & - i \int \mathrm{d}t \langle \phi_f^T \psi_f^T | V_{Pe} G_{of} V_T | \phi_i^T \psi_i^P \rangle \end{aligned} \tag{3.4}$$

where the first integral is the coherent part and the second integral the incoherent part. Again, the term with $V_{Pe} G_{of} V_{Pe}$ is dropped because of its proportionality to the small overlap $\langle \psi_f^P | \psi_i^P \rangle$.

a) Elastic contribution to the EIA

In the electron impact approximation only the first-order term in (3.3) is retained. Neglecting the contribution from the overlap $\langle \psi_f^T | \psi_i^P \rangle$, one is left with the Brinkman-Kramers formula for single electron capture

$$\begin{aligned} a_{fi}^{\mathrm{EIA,\,el}} = & -i \int \mathrm{d}t \langle \psi_f^T | V_T | \psi_i^P \rangle \\ = & -i \int \mathrm{d}t \int \mathrm{d}\mathbf{k}\, \mathrm{e}^{-\mathrm{i}\mathbf{k}\mathbf{R}} \mathrm{e}^{\mathrm{i}(\Delta\varepsilon_{fi} + v^2/2)t} \\ & \times \langle \psi_f^T(\mathbf{r}_T) | V_T(\mathbf{r}_T) | \mathbf{k}^T \rangle \varphi_i^P(\mathbf{k} - \mathbf{v}) \end{aligned} \tag{3.5}$$

where $|\mathbf{k}^T\rangle = (2\pi)^{-3/2} \exp(\mathrm{i}\mathbf{k}\mathbf{r}_T)$, $\Delta\varepsilon_{fi} = E_f - \varepsilon_i^P$ with $E_f = k_f^2/2$ and φ_i^P the Fourier transform of ψ_i^P. A detailed account of the EIA has been given earlier [11], and we mention only the approximations involved. First, the matrix element of V_T is replaced by the elastic scattering amplitude $f(k, \theta)$

$$\begin{aligned} \langle \psi_f^T | V_T | \mathbf{k}^T \rangle = & \langle \mathbf{k}_f^T | V_T | \psi_{\mathbf{k}}^T \rangle \\ \approx & -\frac{1}{(2\pi)^2} f(k, \theta_{\mathbf{k}, \mathbf{k}_f}) \end{aligned} \tag{3.6}$$

where $\theta_{\mathbf{k}, \mathbf{k}_f}$ is the angle between $\mathbf{k}$ and $\mathbf{k}_f$. This on-shell approximation is exact for $k = k_f$ and reasonable in the peak region of the cross section where $k - k_f$ is small. Secondly, a peaking approximation is applied which casts the EIA into the simple product form composed of the cross section $\mathrm{d}\sigma_e/\mathrm{d}\Omega = |f|^2$ for elastic electron scattering on the target field, and the Compton profile J_i which accounts for the momentum distribution of the initial electronic state [11]

$$\begin{aligned} & \frac{\mathrm{d}^2 \sigma^{\mathrm{EIA,\,el}}}{\mathrm{d}E_f \mathrm{d}\Omega_f} = \frac{k_f}{v^2} J_i(k_z - v) \frac{\mathrm{d}\sigma_e}{\mathrm{d}\Omega}(k_z, \vartheta_f) \\ & k_z = (\Delta\varepsilon_{fi} + v^2/2)/v \end{aligned} \tag{3.7}$$

where $\vartheta_f = \sphericalangle(\mathbf{k}_f, \mathbf{v})$ is the emission angle of the electron.

b) Inelastic contribution to the EIA

The inelastic contribution consists of the incoherent term of a_{fi}^{in} from (3.4). Its evaluation proceeds in the same way that has been used for the second Born term [4]. G_{of} is handled by introducing a complete set of intermediate eigenstates to H_{of}, $\psi_n^T * \phi_n^T$, and the quantities related to the projectile rest frame, V_{Pe} and ψ_i^P, are Fourier transformed. One obtains

$$\begin{aligned} a_{fi}^{\mathrm{EIA,\,in}} = & \frac{iZ_P}{\pi} \int \mathrm{d}\mathbf{q}\, \delta(\Delta E_{fi}^T + \Delta\varepsilon_{fi} + v^2/2 - \mathbf{q}\mathbf{v}) \mathrm{e}^{-\mathrm{i}\mathbf{q}\mathbf{b}} \\ & \times \int \frac{\mathrm{d}\mathbf{s}}{s^2} \frac{1}{\Delta E_{fi}^T - \mathbf{s}\mathbf{v} + i\varepsilon} \langle \psi_f^T(\mathbf{r}_T) | V_T | (\mathbf{q} - \mathbf{s})^T \rangle \\ & \times \varphi_i^P(\mathbf{q} - \mathbf{s} - \mathbf{v}) \langle \phi_f^T | \sum_{n=1}^{N} \mathrm{e}^{\mathrm{i}\mathbf{s}\mathbf{r}_{nT}} | \phi_i^T \rangle \end{aligned} \tag{3.8}$$

where $\Delta E_{fi}^T = E_f^T - E_i^T$ and $\Delta\varepsilon_{fi} = E_f - \varepsilon_i^P$. The same matrix element which enters into the elastic EIA transition amplitude (3.5), $\langle \psi_f^T | V_T | \psi_i^P \rangle$, appears in the inelastic EIA amplitude (in the form given by the second line of (3.5)), and is folded with the matrix element for target excitation. Hence, (3.5) together with (3.8) forms a consistent theory.

In order to cast the inelastic contribution to the electron loss cross section into the form (2.6), a peaking approximation is necessary like in the $B2$ theory. Since for light projectiles, φ_i^P is strongly peaked at $\mathbf{q} - \mathbf{s} - \mathbf{v} = 0$, we fix the components of $\mathbf{s}$ perpendicular to $\mathbf{v}$ by $\mathbf{s}_\perp = \mathbf{q}_\perp$ in the target excitation matrix element and also in the matrix element of V_T, assuming they are smoothly varying quantities as compared to the remainder of the integrand. This 'transverse' peaking approximation is similar to the one used in the elastic part of the EIA. In order to eliminate completely the dependence of the target excitation matrix element on the integration variable $\mathbf{s}$, a full peaking is needed for this matrix element. Since $s_z = \Delta E_{fi}^T / v \equiv s_0$ is strongly selected by the energy denominator, we approximate

$$a_{fi}^{\mathrm{EIA,\,in}} = -\frac{i}{\pi}\int \mathrm{d}\mathbf{q}\,\delta(\Delta E_{fi}^{T}+\Delta\varepsilon_{fi}+v^2/2-\mathbf{qv})\,\mathrm{e}^{-i\mathbf{qb}}$$
$$\times\langle\phi_f^T|\sum_{n=1}^{N}\mathrm{e}^{i\mathbf{q}_2\mathbf{r}_{nT}}M^{\mathrm{inc,\,EIA}}(\mathbf{q})|\phi_i^T\rangle$$

$$M^{\mathrm{inc,\,EIA}}(\mathbf{q}) = -Z_P\int_{-\infty}^{\infty}\mathrm{d}s_z\,\frac{1}{\Delta E_{fi}^{T}-s_z v+i\varepsilon}$$
$$\times\langle\psi_f^T(\mathbf{r}_T)|\,V_T|(q_z-s_z)\mathbf{e}_z^T\rangle$$
$$\times\int\mathrm{d}\mathbf{s}_\perp\,\frac{1}{s^2}\,\varphi_i^P(\mathbf{q}-\mathbf{s}-\mathbf{v}) \qquad (3.9)$$

with $\mathbf{q}_2=\mathbf{q}_\perp+s_0\mathbf{e}_z$. For hydrogenlike states, the integral over $\mathbf{s}_\perp$ can be performed analytically. Applying the on-shell approximation (3.6), one obtains for an initial $1s$ state

$$M^{\mathrm{inc,\,EIA}}(\mathbf{q}) = \frac{Z_P^{7/2}}{\sqrt{2}\,\pi^2}\int_{-\infty}^{\infty}\mathrm{d}s_z\,\frac{1}{\Delta E_{fi}^{T}-s_z v+i\varepsilon}$$
$$\times f(|q_z-s_z|,\vartheta_f)\,I_i(s_z,\mathbf{q})$$

$$I_i(s_z,\mathbf{q}) = \frac{1}{\beta}\left(\frac{q_\perp^2+s_z^2}{b_0^2}-1\right) \qquad (3.10)$$
$$-\frac{\alpha}{2\beta^{3/2}}\ln\frac{2\sqrt{\beta}\,(q_\perp^2+s_z^2)+2\beta+\alpha b_0^2}{b_0^2(2\sqrt{\beta}+\alpha)}$$

$$b_0^2 = Z_P^2+(s_z-q_z+v)^2$$

$$\alpha = 2(s_z^2-q_\perp^2-b_0^2),\qquad \beta=(s_z^2+q_\perp^2-b_0^2)^2+4q_\perp^2 b_0^2.$$

The doubly differential cross section for the inelastic EIA contribution is obtained from integrating the absolute square of (3.9) over impact paramters and summing over the final target states. The result is (2.6) with $\Delta E_{fi}=\Delta E_{fi}^{T}+\Delta\varepsilon_{fi}+v^2/2$, $M^{\mathrm{coh}}=0$ and M^{inc} given by (3.10). Applying the Hartley-Walters closure (2.9) and making use of the fact that neither $M^{\mathrm{inc,\,EIA}}$ nor the form factors S_{in}, F_{el} and $\bar{S}$ depend on the azimuthal angle of $\mathbf{q}$, this integral becomes trivial and the cross section is given by

$$\frac{\mathrm{d}^2\sigma^{\mathrm{EIA,\,in}}}{\mathrm{d}E_f\mathrm{d}\Omega_f} = \frac{8\pi k_f}{v^2}\int_0^{\infty}\kappa_T^2\,\mathrm{d}\kappa_T$$
$$\times\int_{q_{\min}(\kappa_T)}^{\infty}q\,\mathrm{d}q\,S_{\mathrm{in}}(q_2)\,|M^{\mathrm{inc,\,EIA}}(\mathbf{q})|^2$$
$$\times\frac{\bar{G}(\kappa_T,q_2)}{\bar{S}(q_2)} \qquad (3.11)$$

with $\bar{G}$ and $\bar{S}$ from (2.10) and (2.11), $q_2=(q^2\sin^2\vartheta_q+s_0^2)^{1/2}$, $s_0=(I^T+\kappa_T^2/2)/v$, $q_{\min}(\kappa_T)=(I^T+\kappa_T^2/2+\Delta\varepsilon_{fi}+v^2/2)/v$, and the polar angle of $\mathbf{q}$ defined by $\cos\vartheta_q=q_{\min}(\kappa_T)/q$.

4. The impulse approximation (IA)

The impulse approximation is obtained by collecting all first- and second-order terms which were defined in the beginning of Sect. 3. From this point of view the IA should be considered as an improvement over the EIA; however, the choice of propagation in the projectile field (the prior form of the IA) restricts its application to systems with $Z_T\leqq Z_P$ as in the case of the second-order Born approximation.

a) Elastic contribution to the IA

The elastic IA transition amplitude is the on-shell approximation to a_{fi}^{el} given in (3.3). Inserting a complete set of eigenstates to $H_{oi}-V_{Po}$, $|\phi_n^T{*}\mathbf{k}^P\rangle$, where $|\mathbf{k}^P\rangle$ is a plane wave with momentum $\mathbf{k}$ in the projectile frame, and making the approximation $(1+V_{Po}G_{oi})|\phi_n^T\mathbf{k}^P\rangle \approx|\phi_n^T\psi_{\mathbf{k}}^P\rangle$ with $\psi_{\mathbf{k}}^P$ an (on-shell) projectile scattering state, one obtains from (3.3)

$$a_{fi}^{\mathrm{IA,\,el}} = -i\int\mathrm{d}t\int\mathrm{d}\mathbf{k}\langle\psi_f^T|\mathbf{k}^P\rangle\langle\psi_{\mathbf{k}}^P|\,V_T|\,\psi_i^P\rangle. \qquad (4.1)$$

It is easily seen that in this expression, the replacement of $V_{ee}+V_{eT}$ by V_T is exact. V_{Pe} does not contribute because ψ_i^P and $\psi_{\mathbf{k}}^P$ are orthogonal. Introducing the Fourier transform $\tilde{V}_T$ of the effective target field, one obtains with $\mathbf{k}_0=\mathbf{k}+\mathbf{v}$

$$a_{fi}^{\mathrm{IA,\,el}} = -\frac{i}{\pi}\int\mathrm{d}\mathbf{q}\,\delta(\Delta\varepsilon_{fi}-v^2/2-\mathbf{qv})$$
$$\times\mathrm{e}^{-i\mathbf{qb}}M_{fi}^{\mathrm{IA,\,el}}(\mathbf{q}) \qquad (4.2)$$

$$M_{fi}^{\mathrm{IA,\,el}}(\mathbf{q}) = \sqrt{\frac{\pi}{2}}\int\mathrm{d}\mathbf{k}_0\,\varphi_f^{T*}(\mathbf{k}_0)\,\tilde{V}_T(\mathbf{k}_0-\mathbf{v}-\mathbf{q})$$
$$\times\langle\psi_{\mathbf{k}_0-\mathbf{v}}^P|\,\mathrm{e}^{i(\mathbf{k}_0-\mathbf{v}-\mathbf{q})\mathbf{r}_P}|\,\psi_i^P(\mathbf{r}_P)\rangle.$$

For the evaluation of the $\mathbf{k}_0$ integral, a transverse peaking approximation is made like in the case of the EIA, relying on the assumption that the Fourier transformed final state, φ_f^T, is strongly peaked at $\mathbf{k}_0=\mathbf{k}_f$. However, the peaking approximation is not so well justified as for the EIA, because φ_f^T, being eigenfunction of a fully screened potential, has a rather broad momentum distribution [18]. We have found it convenient to separate $\varphi_f^T(\mathbf{k}_0)$ into the plane-wave contribution, $\delta(\mathbf{k}_f-\mathbf{k}_0)$, and a finite remainder, a procedure which is allowed for short-range potentials V_T. In the remainder, both $\tilde{V}_T$ and the projectile ionisation matrix element are taken outside the $\mathbf{k}_{0\perp}$ integral at a fixed value $\mathbf{p}_{0\perp}$. With $\mathbf{p}\equiv\mathbf{p}_{0\perp}+k_{0z}\mathbf{e}_z$, one obtains

$$M_{fi}^{\mathrm{IA,\,el}}(\mathbf{q}) \approx M_{fi}^{B1,\,\mathrm{el}}+\sqrt{\frac{\pi}{2}}\int_{-\infty}^{\infty}\mathrm{d}k_{0z}\,\tilde{V}_T(\mathbf{p}-\mathbf{v}-\mathbf{q})$$
$$\times\langle\psi_{\mathbf{p}-\mathbf{v}}^P|\,\mathrm{e}^{i(\mathbf{p}-\mathbf{v}-\mathbf{q})\mathbf{r}_P}|\,\psi_i^P(\mathbf{r}_P)\rangle$$
$$\times\int\mathrm{d}\mathbf{k}_{0\perp}\,\tilde{\varphi}_f^{T*}(\mathbf{k}_0)$$

$$M_{fi}^{B1,\,\mathrm{el}} = \sqrt{\frac{\pi}{2}}\,\tilde{V}_T(\mathbf{k}_f-\mathbf{v}-\mathbf{q}) \times\langle\psi^P_{\mathbf{k}_f-\mathbf{v}}|\,\mathrm{e}^{\mathrm{i}(\mathbf{k}_f-\mathbf{v}-\mathbf{q})\mathbf{r}_P}|\,\psi_i^P(\mathbf{r}_P)\rangle \tag{4.3}$$

where $\tilde{\varphi}_f^T(\mathbf{k}_0)=\varphi_f^T(\mathbf{k}_0)-\delta(\mathbf{k}_f-\mathbf{k}_0)$ and $M_{fi}^{B1,\,\mathrm{el}}$ inserted into (4.2) is identical to the first-order Born contribution to the transition amplitude (the first term in $a_{fi}^{B2,\,\mathrm{el}}$ from (2.5) up to an irrelevant phase). From a detailed analysis of $\int \mathrm{d}\mathbf{k}_{0\perp}\,\tilde{\varphi}_f^{T^*}(\mathbf{k}_0)$ [18] we have chosen $\mathbf{p}_{0\perp}=\mathbf{k}_{f\perp}$ in the vicinity of $k_{0z}=k_{fz}$, and $p_{0\perp}=0$ elsewhere. Taken into consideration that $\tilde{V}_T$ and the ionisation matrix element are weakly dependent on $\mathbf{p}$ and in addition functions of the second integration variable $\mathbf{q}$, the peaking approximation should not lead to serious deficiencies. With the help of (4.3), the elastic contribution to the doubly differential loss cross section is calculated from

$$\frac{\mathrm{d}^2\sigma^{\mathrm{IA,\,el}}}{\mathrm{d}E_f\mathrm{d}\Omega_f}=\frac{8k_f}{v^2}\int_{\tilde{q}_{\min}}^{\infty} q\,\mathrm{d}q\int_0^{\pi}\mathrm{d}\varphi_q\,|M_{fi}^{\mathrm{IA,\,el}}(\mathbf{q})|^2 \tag{4.4}$$

where $\tilde{q}_{\min}=|\Delta\varepsilon_{fi}-v^2/2|/v$, and the polar angle is obtained from $\cos\vartheta_q=(\Delta\varepsilon_{fi}-v^2/2)/(qv)$.

b) Inelastic contribution to the IA

The incoherent part of a_{fi}^{in} from (3.4) has already been discussed, and it remains to evaluate the coherent term. Since this term has the same structure as the corresponding elastic term a_{fi}^{el}, the same steps are taken as before. One obtains

$$a_{fi}^{\mathrm{IA,\,coh}}=-i\int\mathrm{d}t\int\mathrm{d}\mathbf{k}\langle\psi_f^T|\,\mathbf{k}^P\rangle \times\langle\phi_f^T\psi^P_{\mathbf{k}}|\,V_{ee}|\,\phi_i^T\psi_i^P\rangle \tag{4.5}$$

because V_{ee} is the only part of V_i which can induce two-particle transitions. Fourier transforming V_{ee} leads to

$$a_{fi}^{\mathrm{IA,\,coh}}=-\frac{i}{\pi}\int\mathrm{d}\mathbf{q}\,\delta(\Delta E_{fi}^T+\Delta\varepsilon_{fi}+v^2/2-\mathbf{q}\mathbf{v}) \times\mathrm{e}^{-\mathrm{i}\mathbf{q}\mathbf{b}}\int\frac{\mathrm{d}\mathbf{k}_0}{(\mathbf{k}_0-\mathbf{q})^2}\,\varphi_f^{T^*}(\mathbf{k}_0) \times\langle\psi^P_{\mathbf{k}_0-\mathbf{v}}|\,\mathrm{e}^{\mathrm{i}(\mathbf{k}_0-\mathbf{q})\mathbf{r}_P}|\,\psi_i^P(\mathbf{r}_P)\rangle \times\langle\phi_f^T|\sum_{n=1}^{N}\mathrm{e}^{-\mathrm{i}(\mathbf{k}_0-\mathbf{q})\mathbf{r}_{nT}}|\,\phi_i^T\rangle\,. \tag{4.6}$$

This expression is again evaluated with the help of the peaking approximation. Since the Fourier transform of the pure Coulomb field V_{ee} is strongly momentum dependent, care must be taken that also with the peaking approximation, the $\mathrm{d}\mathbf{k}_0$-integrand remains finite at $\mathbf{k}_0=\mathbf{q}$ (each matrix element in (4.6) is proportional to $\mathbf{k}_0-\mathbf{q}$ since the wavefunctions are orthogonal). Therefore, the transverse peaking approximation $\mathbf{k}_{0\perp}=\mathbf{k}_{f\perp}$ is made in the projectile matrix element multiplied by $|\mathbf{k}_0-\mathbf{q}|^{-1}$ and the full peaking approximation $\mathbf{k}_0=\mathbf{k}_f$ in the other terms. One obtains with $\mathbf{p}\equiv\mathbf{k}_{f\perp}+k_{0z}\mathbf{e}_z$

$$a_{fi}^{\mathrm{IA,\,coh}}=-\frac{i}{\pi}\int\mathrm{d}\mathbf{q}\,\delta(\Delta E_{fi}^T+\Delta\varepsilon_{fi}+v^2/2-\mathbf{q}\mathbf{v}) \times\mathrm{e}^{-\mathrm{i}\mathbf{q}\mathbf{b}}\langle\phi_f^T|\sum_{n=1}^{N}\mathrm{e}^{\mathrm{i}\mathbf{q}_1\mathbf{r}_{nT}}M^{\mathrm{coh,\,IA}}(\mathbf{q})|\,\phi_i^T\rangle$$

$$M^{\mathrm{coh,\,IA}}(\mathbf{q})=\frac{1}{|\mathbf{k}_f-\mathbf{q}|}\int_{-\infty}^{\infty}\mathrm{d}k_{0z}\,\frac{1}{|\mathbf{p}-\mathbf{q}|} \times\langle\psi^P_{\mathbf{p}-\mathbf{v}}|\,\mathrm{e}^{\mathrm{i}(\mathbf{p}-\mathbf{q})\mathbf{r}_P}|\,\psi_i^P(\mathbf{r}_P)\rangle \times[\delta(k_{0z}-k_{fz})+\int\mathrm{d}\mathbf{k}_{0\perp}\,\tilde{\varphi}_f^{T^*}(\mathbf{k}_0)] \tag{4.7}$$

where $\mathbf{q}_1=\mathbf{q}-\mathbf{k}_f$. The term proportional to $\delta(k_{0z}-k_{fz})$ coincides again with the first-order Born approximation (the first term in $a_{fi}^{B2,\,\mathrm{in}}$ from (2.5)). In order to obtain the complete inelastic transition amplitude, the incoherent part from (3.9) has to be added:

$$a_{fi}^{\mathrm{IA,\,in}}=a_{fi}^{\mathrm{EIA,\,in}}+a_{fi}^{\mathrm{IA,\,coh}}. \tag{4.8}$$

The doubly differential cross section $\mathrm{d}^2\sigma^{\mathrm{IA,\,in}}/\mathrm{d}E_f\mathrm{d}\Omega_f$ is obtained from the formulae (2.6)–(2.11) with the substitution $M^{\mathrm{coh}}(\mathbf{q})\to M^{\mathrm{coh,\,IA}}$ from (4.7), $M^{\mathrm{inc}}(\mathbf{q})\to M^{\mathrm{inc,\,EIA}}$ from (3.9), $\mathbf{q}_1=\mathbf{q}-\mathbf{k}_f$, $\mathbf{q}_2=\mathbf{q}_\perp+(\Delta E_{fi}^T/v)\mathbf{e}_z$ and $\Delta E_{fi}=\Delta E_{fi}^T+\Delta\varepsilon_{fi}+v^2/2$. As q_1 depends explicitly on the azimuthal angle of $\mathbf{q}$, the integral over $\mathbf{q}$ can only be reduced to a two-dimensional integral which has to be carried out numerically.

5. Numerical details

For the evaluation of the electron loss cross section in the electron impact approximation and the impulse approximation, knowledge of the target continuum eigenfunctions, their Fourier transform and the scattering amplitude is required. For simplification, the target atom is approximated by an effective one-electron potential. This is a reasonable approximation for high-energy electron scattering where exchange effects are of minor importance and orthogonality to the bound electronic states need not be considered [19]. The electronic scattering state is represented in terms of partial waves, and the radial part $R_l(k,r)$ of the l^{th} partial wave is obtained from the Schrödinger equation

$$\left(\frac{\mathrm{d}^2}{\mathrm{d}r^2}+k^2-\frac{l(l+1)}{r^2}-2V(r)\right)R_l(k,r)=0 \tag{5.1}$$

where k is the electronic momentum. The potential consists of the static and the polarisation field [11, 19]

$$V(r)=V_T(r)+V_{\mathrm{pol}}$$

$$V_T(r)=-\frac{Z_T}{r}\sum_{i=1}^{2}(a_i\mathrm{e}^{-b_ir}+\alpha_i r\,\mathrm{e}^{-\beta_i r}) \tag{5.2}$$

$$V_{\mathrm{pol}}=-\frac{\alpha r^2}{2(r^2+\mathrm{d}^2)^3},\qquad \mathrm{d}=\frac{3\bar{k}}{8\Delta},$$

$$\bar{k}=\begin{cases}k_0, & k\leqq k_0\\ k, & k>k_0\end{cases}$$

The static field $V_T(r)$ has been fitted to the target Hartree Fock potential where a_i, b_i, α_i and β_i are the fit parameters [17]. In the polarization field V_{pol}, α is the dipole polarizability and Δ the mean target excitation energy (for He, $\alpha = 1.38414$, $\Delta = 1.22$ a.u.). For large electron momenta ($k \gtrsim (3\Delta)^{1/2}$), the cutoff constant d is proportional to k [19]. This will be the case for the dominant contribution to the cross section because the collision velocity is large and $k \sim v$ (see e.g. (3.7)). However, for the inelastic EIA cross section, R_l is also needed for small values of k. In that case, one would have to solve a self-consistent differential equation including exchange [20]. Since the small-k contribution is of minor importance as discussed below, we have made a crude approximation: $R_l(k, r)$ has also been calculated from (5.1) with (5.2), using a constant cutoff d in V_{pol}. The value $k_0 = 1.1$ (for He) has been taken from an earlier fit to accurate low-energy phase shifts [21].

For the impulse approximation, the integral over the transverse components of the scattering state in momentum space is needed. Within the partial wave representation, this double integral can be performed analytically [18]. Hence, only the r integral inherent in the Fourier transformation of the scattering state has to be calculated numerically. This can be done simultaneously with the integration of the Schrödinger equation (5.1).

The scattering amplitude is readily calculated with the help of the phase shifts δ_l, which are determined from the large-r behaviour of the radial functions $R_l(k, r)$

$$f(k, \theta) = \frac{1}{k} \sum_{l=0}^{l_{\max}} (2l+1) P_l(\cos\theta) \, e^{i\delta_l} \sin\delta_l \tag{5.3}$$

where P_l is a Legendre polynomial, and the cutoff $l_{\max}$ is taken sufficiently large to obtain convergence ($l_{\max} \approx 16$ for He). Making use of the fact that for $V(r) = 0$, $\delta_l \to 0$ for $r \to \infty$, accurate values of δ_l are obtained already at moderate r if (5.1) is first solved with (5.2) and subsequently with $V(r) = 0$. δ_l is then equal to the difference of the corresponding phase shifts at fixed r.

Since the evaluation of the scattering amplitude and of the momentum-space scattering state is rather time-consuming, these functions are calculated prior to the evaluation of the cross sections on a grid of mesh points, and interpolated subsequently with a spline interpolation routine. In the case of EIA, this is made possible by the variable transform in (3.10) $s_z' = s_z - s_0$, such that the argument of the scattering amplitude, $q_z - s_z = \Delta\varepsilon_{fi}/v + v/2 - s_z'$, only depends on s_z' but not on the target excitation energy $\kappa_T^2/2$. The singularity in the s_z' integral at $s_z' = 0$ is readily handled by means of the decomposition

$$\int_{-\infty}^{\infty} ds_z' \frac{1}{-s_z' v + i\varepsilon} F(s_z')$$

$$= -\int_{-\infty}^{\infty} ds_z' [F(s_z') - F(0)] \frac{1}{s_z' v} - \frac{i\pi}{v} F(0)$$

$$F(s_z') = f(|k_z - s_z'|, \vartheta_f) I_i(s_z' + s_0, \mathbf{q}) \tag{5.4}$$

with k_z defined in (3.7). Since I_i rapidly decreases with $|s_z'|$, it is obvious from (5.4) that the dominant contribution to the inelastic EIA cross section comes from the region around $s_z' = 0$. At this value, the particular scattering amplitude $f(k_z, \vartheta_f)$ enters into the formula, which also determines the elastic EIA cross section (3.7).

The ionisation matrix element appearing in the IA ((4.3) and (4.7)) can be calculated analytically for hydrogenic states (see, e.g. [4]). In addition to the square root singularity at $\mathbf{p} = \mathbf{v}$ from the normalisation constant of the Coulomb wave $\psi^P_{\mathbf{p}-\mathbf{v}}$, there appear two logarithmic singularities at $k_{oz} = \pm k_f$ from the Fourier transform of the scattering state [18]. These singularities are readily handled by splitting the k_{oz} integral and making a logarithmic variable transform (except in the region of the maximum at $k_{oz} = k_{fz}$).

6. Results

The total loss cross section is calculated from the sum of the elastic and the inelastic contribution

$$\frac{d^2\sigma}{dE_f d\Omega_f} = \frac{d^2\sigma^{\text{el}}}{dE_f d\Omega_f} + \frac{d^2\sigma^{\text{in}}}{dE_f d\Omega_f} \tag{6.1}$$

within the three theories presented above, the second-order Born approximation, the electron impact approximation and the impulse approximation. Comparison is made with the coincidence data of DuBois and Manson

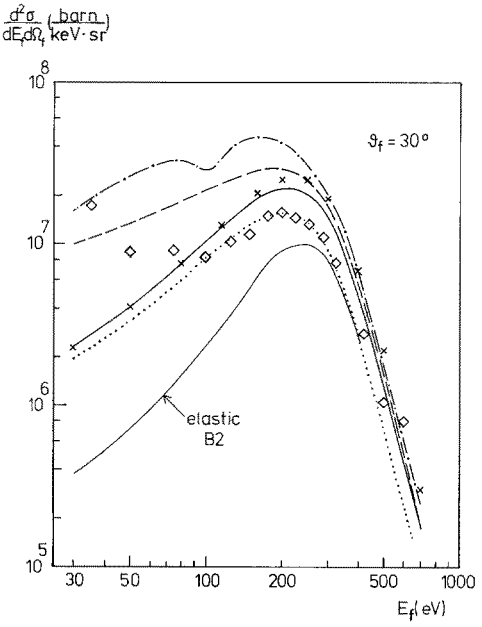

Fig. 2. Doubly differential loss cross section for 0.5 MeV/N $He^+ + He$ collisions as a function of electron energy E_f at an emission angle of 30°. Shown are results from the second Born approximation with the Hartley-Walters closure (——) and the conventional closure (×), the first Born approximation (· · · · · · ·), the EIA (- - - -) and the impulse approximation (—·—·—·—), all with the Hartley-Walters closure. Shown is also the elastic $B2$ contribution (———). The experimental data (◇) are taken from DuBois and Manson [5]

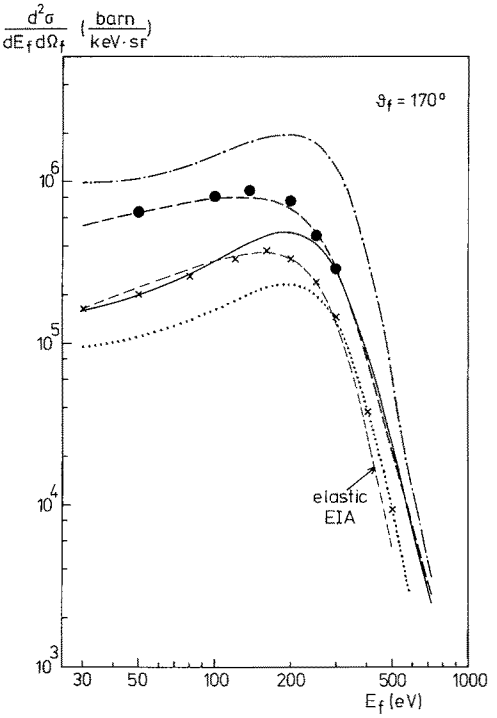

Fig. 3. Doubly differential loss cross section for 0.5 MeV/N $He^+ + He$ collisions as a function of electron energy E_f at an emission angle of 170°. The theoretical curves have the same meaning as in Fig. 2, except for the elastic EIA contribution (– – –). The experimental data (●) are taken from Kövér et al. [12]

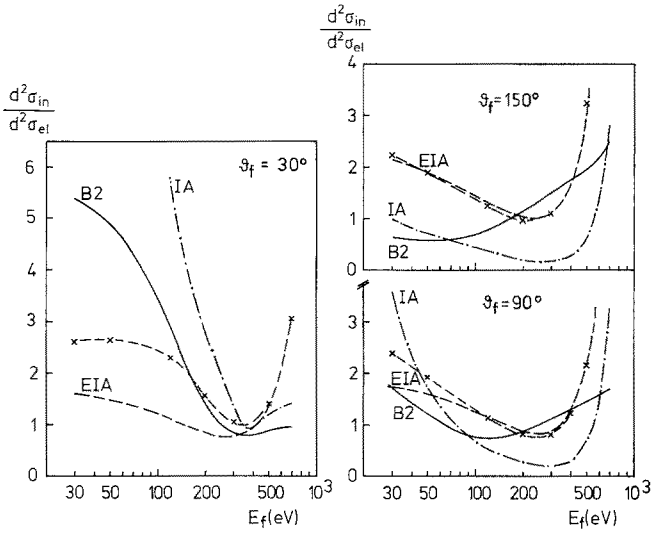

Fig. 4. Ratio $d\sigma^{in}/d\sigma^{el}$ of the inelastic and the elastic contribution to the doubly differential loss cross section for 0.5 MeV/N $He^+ + He$ collisions at emission angles 30°, 90° and 150°. Shown are calculations within the second Born (———), the EIA (– – –) and the impulse approximation (– · – · –). Also shown is a modified EIA ratio where in the inelastic part, the first-order Born term is added coherently (× – – – ×)

[5] and Heil et al. [7], and with the singles data of Kövér et al. [12]. Figures 2 and 3 show the energy distribution of electrons emitted in 0.5 MeV/N $He^+ + He$ collisions at the two angles $\vartheta_f = 30°$ and 170°. At forward angles, the Born approximation gives the best description of the data. Inclusion of the second Born term increases the cross section in the peak region by ~40% at $\vartheta_f = 30°$, but by a factor of 2 at $\vartheta_f \gtrsim 90°$, which is considerably more than in the cusp region (10% [4]) at this particular collision velocity. In order to test the accuracy of the closure approximation for the inelastic contribution to the cross section, the second-order Born theory has been calculated with the Hartley-Walters closure (2.9) as well as with the conventional closure approximation. At small electron energies the difference is rather small, while at energies beyond the peak, particularly at backward emission angles, there are considerable deviations between the two approximations (up to a factor of 2). In this context it should be recalled that the choice $\Delta E_{fi}^T \to I^T + \kappa_f^2/2$ in the conventional closure approximation is derived from a mere consideration of the electron-electron coupling where it is assumed that the two electrons acquire an equal amount of momentum [15]. With increasing momentum transfer to the projectile electron (i.e. for increasing ϑ_f or E_f beyond the peak), the coherent ionisation looses importance as compared to the incoherent (double-interaction) ionisation, such that the Hartley-Walters closure which models the true target energy levels beyond threshold is more reliable than the conventional closure.

At backward emission angles, the electron impact approximation is superior to the Born approximation in explaining the experimental data. This theory does not include the coherent ionisation. In order to check possible deficiencies of the EIA, the coherent ionisation has been accounted for by using the IA formula (4.8) but retaining only the δ-contribution from (4.7). Although this addition of the first Born term (with a *projectile* final state) is not quite consistent, it gives an estimate of the importance of the coherent ionisation as compared to the incoherent ionisation. It follows from Fig. 4 that for small ϑ_f the inelastic loss cross section is enhanced as compared to EIA (up to a factor of 2 at $\vartheta_f = 30°$), but there is little effect at backward angles. Hence, in the validity regime of the EIA, the neglect of the coherent ionisation is a reasonable approximation.

While the coherent ionisation must be taken into account at forward angles, consideration of the incoherent projectile-target ionisation is important at all angles. If only the elastic part of the loss cross section were accounted for, the experimental data were underestimated considerably, both by $B2$ at forward angles and by EIA at backward angles (see Figs. 2, 3). As is evident from Fig. 4 where the ratio between the inelastic and the elastic loss cross section is plotted as a function of energy, the inelastic contribution is particularly large on the outer wings of the loss peak, where it may strongly exceed the elastic part of the loss cross section. This behaviour which is common to all theories may be explained by realising that the momentum transfer required to eject a loosely bound target electron is of similar magnitude (or even smaller) than the momentum which must be absorbed by the projectile electron. Therefore, the probability for the occurrence of double ionisation during the collision is very large.

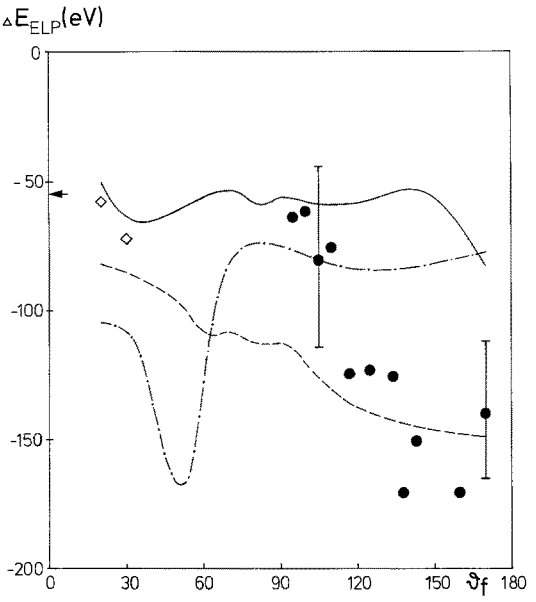

Fig. 5. Shift ΔE_{ELP} of the electron loss peak maximum relative to $v^2/2$ in 0.5 MeV/N $He^+ + He$ collisions as a function of electron emission angle ϑ_f. Shown are the results from $B2$ (———), EIA (– – –) and IA (– · – · –). The arrow denotes the initial-state energy ε_i^P. The experimental data are from DuBois and Manson (◇, [5]) and from Kövér et al. (◆, [12])

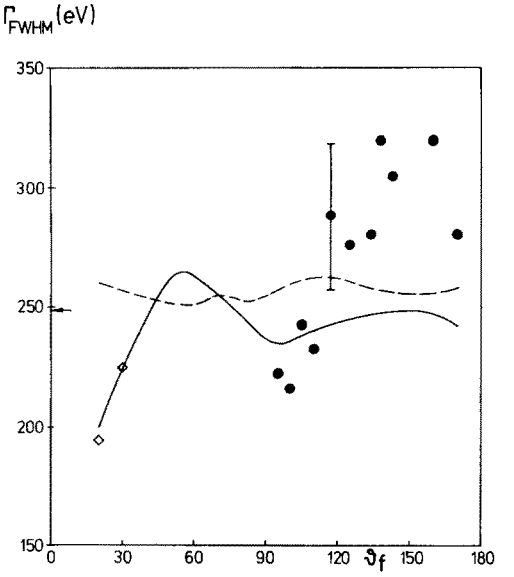

Fig. 6. Full width at half maximum, Γ_{FWHM}, of the electron loss peak from 0.5 MeV/N $He^+ + He$ collisions as a function of emission angle ϑ_f. Shown are results from the second Born approximation (———) and the electron impact approximation (– – –). The arrow denotes the width of the Compton profile from (3.7). The experimental data are taken from DuBois and Manson (◇, [5]) and Kövér et al. (◆, [12])

The presence of the target electrons leads not only to a general enhancement of the loss cross section, but it affects also the position and shape of the loss peak itself. The gross features can be explained by the properties of the projectile alone: from e.g. the formula (3.7) for the elastic EIA it follows that the peak position is determined from the requirement $k_z = v$, i.e. $E_{\max} = v^2/2 + \varepsilon_i^P$, whereas its shape mirrors the momentum distribution of the bound projectile electron as expressed by the Compton profile J_i. The influence of the target electrons which manifests itself not only in the presence of the inelastic loss cross section, but also in the angular and energy dependence of the scattering amplitude, leads to a change of the peak position and width when the emission angle is varied. Figure 5 displays the peak shift $\Delta E_{\mathrm{ELP}} = E_{\max} - v^2/2$ which from the arguments above should be close to ε_i^P. This is approximately true for the second Born approximation but not for the EIA which shows a steadily increasing peak shift with increasing ϑ_f. The wiggles arise from the (nonperturbative) influence of the target atomic field and are the more pronounced, the heavier the target [11]. Wiggles in the backward direction may have been artificially suppressed because calculations for $\vartheta_f > 90°$ have only been performed at a few angles (120°, 150°, 170°), with a smooth interpolation in between. From comparison with experiment, the second Born theory is favoured for $\vartheta_f \lesssim 110°$, while the EIA gives a better description at larger angles.

The influence of the target field on the peak width as a function of angle is displayed in Fig. 6. There is again indication that at angles up to 110°, the second-order Born approximation is appropriate while EIA fails. At larger angles, the two theories give rather similar results. The large deviation between theory and the singles data at backward angles may be due to experimental uncertainties caused by the large background from target ionisation when the peak maximum is shifted to small energies. At a 'critical' angle of ~55°, the $B2$ theory suggests a very broad electron loss peak as compared to adjacent angles. This behaviour is related to the inelastic part of the loss cross section which near the critical angle peaks at much lower energies than the elastic part.

A similar behaviour, supported by experimental data [6, 7] is found for electron loss in $H^0 + He$ collisions [8], where the critical angle is ~30° (Fig. 7). In this figure, the dependence of the loss cross section on the projectile species is shown by selecting H^0 and He^0 projectiles at the same collision energy as was chosen for He^+. For the He^0 projectile, only EIA calculations have been performed, and the following changes have been made in the theory for He^+: *(i)* The hydrogenic initial binding energy is replaced by 0.91795 a.u.. *(ii)* For the initial hydrogenic wavefunction ψ_i^P an effective charge $Z_{P,\mathrm{eff}} = 1.7$ is used. *(iii)* V_{Pe} is replaced by the Hartree-Fock potential for He^+ which means that in (3.9), Z_P/s^2 is replaced by $(Z_P/s^2)(1 - 16Z_P^3/(s^2 + 4Z_P^2)^2)$ with $Z_P = 2$. In the step from (3.9) to (3.10) the transverse peaking approximation ($s_\perp^2 = q_\perp^2$) is also made in this factor multiplying Z_P/s^2. *(iv)* The cross section is enhanced by a factor of 2 due to the presence of two projectile K-shell electrons.

In contrast to the case of 30° $He^+ + He$ (Fig. 2), the loss of the more loosely bound electrons of H^0 and He^0 is not only reasonably well described by the second Born theory, but also by EIA. This means that for a smaller ratio of Z_P/Z_T (or $Z_{P,\mathrm{eff}}/Z_T$), the description of the

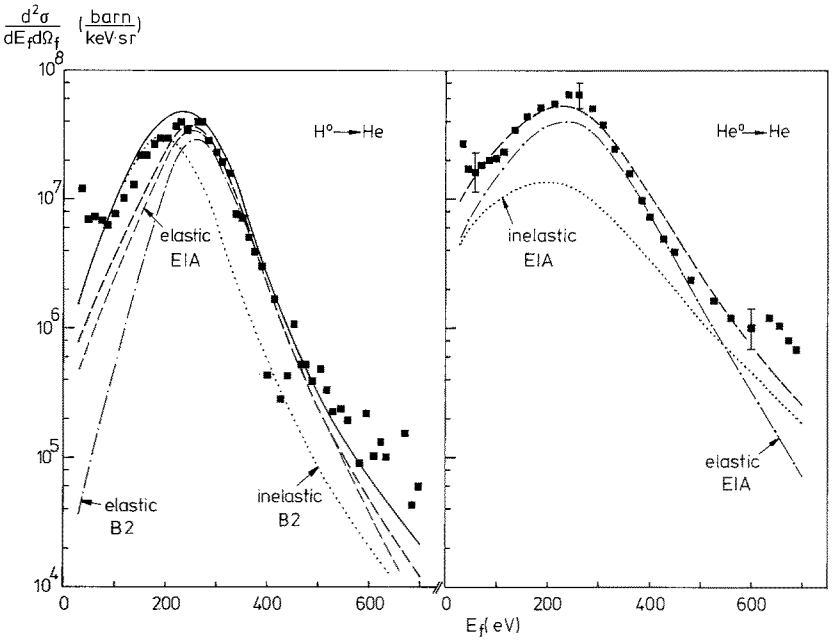

Fig. 7. Doubly differential one-electron loss cross section for 0.5 MeV/N $H^0 + He$ (left) and $He^0 + He$ (right) collisions as a function of electron energy E_f at an emission angle of 30°. Shown are theoretical cross sections within the second Born approximation (———) and the electron impact approximation (– – –), as well as the elastic and the inelastic contributions to $B2$ and EIA. The experimental data are from Heil et al. [7]

emitted electron by a target eigenstate can be applied for considerably smaller angles than in case of $Z_P/Z_T = 1$. The basic difference between the two theories lies in the inelastic contribution: while for $B2$, this contribution gains importance when Z_P is reduced, it is vice versa for EIA. This is so because the electron-electron coupling (which governs $B2$ at forward angles) is the more important as compared to electron-nucleus couplings (which enter into the EIA), the smaller the nuclear charges [8, 22]. Inclusion of the coherent projectile-target ionisation in the EIA would lead to some enhancement on the low-energy side of the loss peak, particularly for the $H^0 + He$ system, improving the agreement with the data.

7. Conclusion

Electron loss spectra from collisions of hydrogen and helium with He have been calculated within three high-velocity perturbative prescriptions, the second-order Born approximation, the electron impact approximation and the prior impulse approximation. Comparison of the shape and position of the electron loss peak with experimental data confirms the conjecture that electrons ejected into the forward hemisphere are predominantly influenced by the projectile field. The second Born theory which accounts for this fact, is in good agreement with the data. At backward emission angles ($\vartheta_f \gtrsim 110°$ for $He^+ + He$), electron loss is preferably described in terms of electron capture to the target continuum. The smaller the ratio between the projectile and target nuclear charges, the more extends the validity of this prescription into the forward hemisphere. The (first-order) EIA theory gives a satisfactory explanation of the data, whereas the prior impulse approximation for electron capture overestimates the experimental spectra at all angles. The failure of this higher-order theory which originally was designed as an improvement on the EIA, may be due to the description of the electronic intermediate states: when the electrons are predominantly influenced by the target field in their final state, this field will also act on their intermediate states, even for symmetric systems like He + He. Hence, an improvement on the EIA is rather expected from a second-Born type theory which includes target intermediate states. Since, however, exact eigenstates to the atomic target field are essential for a proper description of electron loss at the larger emission angles, such a theory is far more intricate than the EIA or prior IA.

We have found that consideration of simultaneous target excitation is very important for electron loss, irrespective of the emission angle and the projectile and target species. This inelastic process not only enhances the peak intensity considerably, but also gives the dominant contribution to low-energy electron emission. Hence, the electron loss peak is shifted to lower energies as compared to the elastic contribution alone, and the peak width is increased, particularly near a critical forward angle which depends on the collision system. There are two contributions to simultaneous target excitation: at small emission angles, the coherent projectile-target ionisation must be taken into consideration. This contribution which is important for small momentum transfers to the projectile electron, increases with decreasing electron energy and emission angles, and also with decreasing nuclear charge of projectile and target. The incoherent projectile-target ionisation, on the other hand, should be included at all angles and is largely dominant for high momentum transfers. Hence, this contribution increases with increasing electron energy and emission angles, and also with increasing projectile and target charges. When calculated within a second-order approximation, the incoherent contribution scales relative to the elastic contribution approximately with $Z_P^2 * Z_T$. This scaling may, however, break down for large Z_P and Z_T, where third- and higher-order terms will have to be included.

I should like to thank O. Heil for many stimulating discussions and for communicating his experimental results prior to publication. I should also like to thank K.O. Groeneveld and his group for the great hospitality during my visits in Frankfurt. Support from the GSI Darmstadt is gratefully acknowledged.

References

1. Briggs, J.S., Drepper, F.: J. Phys. B**11**, 4033 (1978)
2. Knudsen, H., Andersen, L.H., Jensen, K.E.: J. Phys. B**19**, 3341 (1986)
3. Atan, H., Steckelmacher, W., Lucas, M.W.: J. Phys. B**23**, 2579 (1990)
4. Jakubaßa-Amundsen, D.H.: J. Phys. B**23**, 3335 (1990)
5. DuBois, R.D., Manson, S.T.: Phys. Rev. Lett. **57**, 1130 (1986)
6. Heil, O., Dubois, R.D., Maier, R., Kuzel, M., Groeneveld, K.O.: Nucl. Instrum. Methods B**56/57**, 282 (1991)
7. Heil, O., DuBois, R.D., Maier, R., Kuzel, M., Groeneveld, K.O.: Z. Phys. D - Atoms, Molecules and Clusters **21**, 235 (1991)
8. Kahle, M.: Diploma Thesis, University of Munich (1991)
9. Hartley, H.M., Walters, H.R.: J. Phys. B**20**, 1983 (1987)
10. Hartley, H.M., Walters, H.R.: J. Phys. B**20**, 3811 (1987)
11. Jakubaßa, D.H.: J. Phys. B**13**, 2099 (1980)
12. Kövér, Á., Szabó, Gy., Gulyás, L., Tökési, K., Berényi, D., Heil, O., Groeneveld, K.O.: J. Phys. B**21**, 3231 (1988)
13. Dettmann, K., Leibfried, G.: Z. Phys. **218**, 1 (1969)
14. Briggs, J.S.: J. Phys. B**10**, 3075 (1977)
15. Day, M.H.: J. Phys. B**14**, 231 (1981)
16. Briggs, J.S., Taulbjerg, K.: In: Topics in Current Physics. Sellin, J.A. (ed.), vol. 5, p. 105. Berlin, Heidelberg, New York: Springer 1978
17. Strand, T.G., Bonham, R.A.: J. Chem. Phys. **40**, 1686 (1964)
18. Jakubaßa-Amundsen, D.H.: Phys. Lett. A**158**, 129 (1991)
19. Jhanwar, B.L., Khare, S.P., Kumar Jr., A.: J. Phys. B**11**, 887 (1978)
20. Nakanishi, H., Schrader, D.M.: Phys. Rev. A**34**, 1810 (1986)
21. Jakubaßa-Amundsen, D.H.: J. Phys. B**22**, 3989 (1989)
22. Gillespie, G.H.: Phys. Rev. A**18**, 1967 (1978)